Molecular Crystals and Liquid Crystals

Publication details, including instructions for authors and subscription information:
http://www.tandfonline.com/loi/gmcl20

Compression Induced Achiral-Chiral Phase Transition of Monolayers Comprised of Banana-Shaped Achiral Molecules at the Air-Water Interface: Importance of In-plane Nematic Order

Tetsuya Yamamoto [a b], Dai Taguchi [a b], Takaaki Manaka [a] & Mitsumasa Iwamoto [a]

[a] Department of Physical Electronics, Tokyo Institute of Technology, Meguro-ku, Tokyo, Japan

[b] JSPS-fellow, Chiyoda-ku, Tokyo, Japan

Version of record first published: 22 Sep 2010

To cite this article: Tetsuya Yamamoto, Dai Taguchi, Takaaki Manaka & Mitsumasa Iwamoto (2007): Compression Induced Achiral-Chiral Phase Transition of Monolayers Comprised of Banana-Shaped Achiral Molecules at the Air-Water Interface: Importance of In-plane Nematic Order, Molecular Crystals and Liquid Crystals, 479:1, 13/[1051]-31/[1069]

To link to this article: http://dx.doi.org/10.1080/15421400701732365

Mol. Cryst. Liq. Cryst., Vol. 479, pp. 13/[1051]–31/[1069], 2007

ISSN: 1542-1406 print/1563-5287 online
DOI: 10.1080/15421400701732365

Compression Induced Achiral-Chiral Phase Transition of Monolayers Comprised of Banana-Shaped Achiral Molecules at the Air-Water Interface: Importance of In-plane Nematic Order

Tetsuya Yamamoto
Dai Taguchi
Department of Physical Electronics, Tokyo Institute of Technology, Meguro-ku, Tokyo, Japan; JSPS-fellow, Chiyoda-ku, Tokyo, Japan

Takaaki Manaka
Mitsumasa Iwamoto
Department of Physical Electronics, Tokyo Institute of Technology, Meguro-ku, Tokyo, Japan

Monolayers comprised of banana-shaped achiral molecules are modeled taking into account the hard-core repulsive force and electrostatic interaction between constituent molecules and the water surface. The model predicts the achiral-chiral transition of orientational structure along with in-plane nematic ordering during a monolayer compression due to the 2D geometry of monolayers. This model further reveals that in-plane nematic order is established beforehand of the chiral transition since banana-shaped molecules behave as rod-shaped molecules with variable aspect ratio in 2D geometry. It indicates the importance of in-plane nematic order in the achiral-chiral phase transition of monolayers comprised of banana-shaped achiral molecules.

Keywords: banana-shaped achiral molecules; chiral structure; geometry effect; Williams-Bragg approach

PACS Numbers: Codes 68.18.-g and 61.30.cz

I. INTRODUCTION

The physicochemical properties of amphiphile monolayers at the air-water interface have been attracted much attention since the

This work was supported by the Grants-in-Aid for Scientific Research of JSPS.
Address correspondence to Mitsumasa Iwamoto, Department of Physical Electronics, Tokyo Institute of Technology, 2-12-1 S3-33 O-okayama, Meguro-ku, Tokyo 152-8552, Japan. E-mail: iwamoto@ome.pe.titech.ac.jp

preparation technique was developed by Langmuir [1,2]. The structures of monolayers are determined by positional order of molecular head on the water surface and orientational order of molecular tail pointing towards the air. The orientational order parameters $S_n\big(\equiv\langle P_n(\cos\theta)\rangle\big)$ have been introduced to represent the orientational structure of monolayers comprised of rod-shaped molecules as an extension of the orientational order parameter S_2 of nematic liquid crystal [3], where $P_n(\cos\theta)$ is the Legendre polynomial of n-th rank and θ is the tilt angle from the water surface. The non-centrosymmetric structure of monolayers is characterized by the presence of the odd-number-th orientational order parameters, i.e., $S_{2m-1}\neq 0$ $(m = 1, 2, \ldots)$. From the viewpoint of dielectric physics of monolayers, the spontaneous and second order non-linear polarizations are generated from monolayers due to $S_1\neq 0$ and $S_3\neq 0$ [4]. We have developed Maxwell displacement current (MDC) and optical second harmonic generation (SHG) measurements to detect the spontaneous and second order non-linear polarizations, and have measured S_1 and S_3 of monolayers comprised of rod-shaped achiral molecules, e.g., alkyl-cyanobiphenyl homologues [5]. Recently, it has been demonstrated that MDC-SHG measurement is capable of probing the chirality of monolayers comprised of chiral rod-shaped molecules, which originates from the molecular chirality [6,7].

Thus far, we have focused on monolayers comprised of achiral and chiral rod-shaped molecules, where the molecular symmetries are $C_{\infty v}$ and C_∞, respectively. In order to extend our knowledge, we have been studying monolayers comprised of banana-shaped achiral molecules (C_{2v} symmetry) [8–10]. Bulk liquid crystals of banana-shaped achiral molecules have been recognized as one of the most important materials [11–13]. Liquid crystals of banana-shaped molecules form a ferroelectric phase, where banana-shaped achiral molecules are stacked in the smectic-like layer structure (B_2 phase) [12]. The spontaneous polarization generated from each layer originates from the orientational ordering of dipole moment in C_2-axis (ζ-axis in Fig. 1) parallel to the layer plane. On account of the orientational ordering of the molecular long axis (ξ-axis), each layer of B_2 phase lacks mirror symmetry even though it is comprised of achiral components [11,13]. As an extension of molecular chirality, we denote the macroscopic structure without mirror symmetry as chiral in this article. Since it is possible that the chiral structure formation of bulk liquid crystal of banana-shaped achiral molecules is attributed to the structure of banana-shaped molecules at the interface between liquid crystal and substrate, it is important to clarify the orientational structure of banana-shaped molecules at the interface.

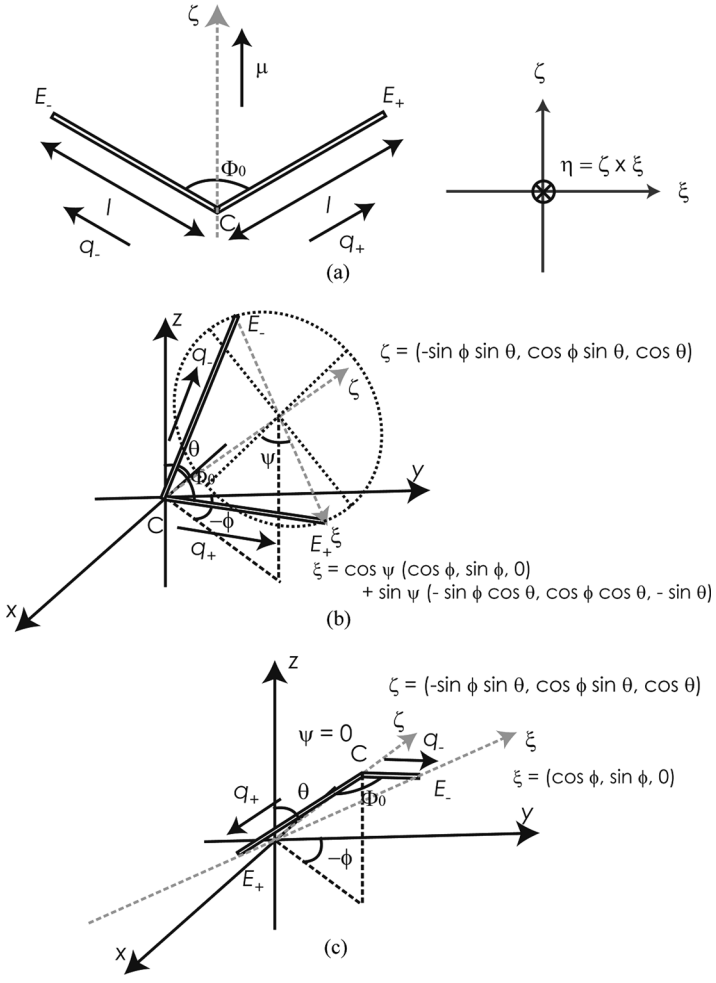

FIGURE 1 (a) Model of banana-shaped molecule and classification of banana-shaped achiral molecules; (b) a type 1 banana-shaped molecule (c) type 2 banana-shaped molecule.

In our previous study, the orientational structure of 1-*butyl*-2,6-*bis*-[2-(4-*dibutylaminophenyl*)-*vinyl*]-*pyridiniumiodide* (M53) monolayers at the air-water interface has been studied by means of MDC-SHG measurement to investigate the formation of chiral structure as an assembly of achiral molecules [8]. Unfortunately, such chirality was not detected from M53 monolayers though MDC-SHG measurements are capable of probing the chirality of monolayers [7]. In order to

clarify this experimental result, we carried out an analysis taking into account the geometrical constraint imposed on the molecular rotation of banana-shaped molecules around ζ-axis (interfacial binding effect) [8]. Amphiphile banana-shaped achiral molecules must possess hydrophobic part either at the end of two legs E_+ and E_- (type 1) or at the connecting part C of two legs (type 2) to float on the water surface (see Figs. 1 (b) and (c)). When the constituent banana-shaped molecules are tilted from the water surface normal ($\theta \neq 0$), a type 1 molecule can rotate around ζ-axis somewhat ($\psi \neq 0$), whereas rotation of a type 2 molecule around ζ-axis is prohibited ($\psi = 0$) owing to the strong hydrophobic repulsive interaction between constituent molecules and water surface. According to Simpson [14], monolayers comprised of banana-shaped achiral molecules can form chiral structure when the orientational distribution of constituent molecules is asymmetric with respect to the twist angle ψ due to the symmetry breaking at the interface. In other words, while there still exists the possibilities that monolayers comprised of type 1 banana-shaped achiral molecules form chiral structure, monolayers comprised of type 2 banana-shaped molecules do not form chiral structure. M53 molecules are classified as type 2 molecules from the result of MDC measurement, i.e., M53 monolayers did not form chiral structure due to the interfacial binding effect. In that analysis, we have shown that the molecular rotation of a type 1 banana-shaped molecules around ζ-axis is possible, but we have not shown that monolayers comprised of type 1 banana-shaped molecules form chiral structure.

Recently, we have analyzed the orientational structure of monolayers comprised of type 1 banana-shaped achiral molecules taking into account the electrostatic interaction between constituent molecules and the water surface, and the hard-core repulsive interaction between constituent molecules [10]. Since constituent banana-shaped achiral molecules are aligned at a 2D surface, we only take into account the hard-core repulsive interaction between the projection of constituent banana-shaped molecules onto the water surface [9]. It has been demonstrated that monolayers comprised of type 1 banana-shaped molecules form chiral structure in the course of the monolayer compression (compression induced chiral symmetry breaking) due to the geometry of molecular alignment in 2D surface on the analogy of Williams-Bragg approach. This analysis also have revealed that the in-plane nematic order, i.e., orientational order with respect to ζ-axis of a constituent molecule, plays an important role in the formation of chiral orientational structure. However, we did not discuss the formation mechanism of in-plane nematic order of monolayers comprised of banana-shaped molecules in this analysis. In the present

study, we have studied the formation of in-plane nematic order of monolayers comprised of type 1 banana-shaped achiral molecules to investigate the importance of in-plane nematic order in the achiral-chiral phase transitions of such monolayers. We briefly review the model of monolayers comprised of type 1 banana-shaped achiral molecules and the mechanism of chiral-achiral phase transition to show why it is necessary to study the in-plane nematic order in sec. II and III. In a manner similar to Onsager's theory of isotropic-nematic phase transition of 3D bulk liquid crystal [15], we consider that the hard-core repulsive interaction is the origin of the in-plane nematic ordering. It is demonstrated that type 1 banana-shaped achiral molecules are viewed as a rod-shaped molecule with variable aspect ratio in 2D geometry and that in-plane nematic order is established in the course of the monolayer compression at larger molecular area than the achiral-chiral phase transition in sec. IV. We conclude our article in sec. V. Since we only discuss monolayers comprised of type 1 banana-shaped molecules in this article, we denote type 1 banana-shaped achiral molecules as just banana-shaped achiral molecules in the following.

II. A STATISTICAL MECHANICAL MODEL OF MONOLAYERS COMPRISED OF BANANA-SHAPED ACHIRAL MOLECULES

In this section, we construct a statistical mechanical model of monolayers comprised of the banana-shaped achiral molecules taking into account the electrostatic Coulomb interaction between the dipole moments of constituent molecules and image dipoles induced at the water surface, and hard-core repulsive interaction between constituent molecules [10]. Figure 1(b) is the model of a type 1 banana-shaped achiral molecules. In the monolayer coordinate system, the orientations of the two legs $\mathbf{q}_+$ and $\mathbf{q}_-$ of the i-th molecule are determined by the tilt angle θ_i, twist angle ψ_i, and tilt azimuth ϕ_i of the i-th molecule (see Fig. 1(b)). A banana-shaped molecule possesses permanent dipole moment in ζ direction due to the symmetry of the model molecule (C_{2v}). We assume that the dipole moment is represented by the sum of dipole moments $\mu_+(=\mu_0\mathbf{q}_+)$ and $\mu_-(=\mu_0\mathbf{q}_-)$ at the two legs of a banana-shaped molecule, where μ_+ and μ_- are comprised of positive charges at the end E_+ and E_- of two legs and negative charges of the connecting portion C of the two legs. The dipole moments at the two legs of constituent molecules induce image dipole moments at the water surface. The electrostatic energy due to the interaction between the dipole moment of the i-th molecule and image dipole at

the water surface is written as [10]

$$V(\theta_i,\psi_i) = -\frac{\mu_0^2}{16\pi l^3\epsilon_0\epsilon_m}\frac{\epsilon_w-1}{\epsilon_w+1}\left(\frac{1}{\cos\frac{\Phi_0}{2}\cos\theta_i - \sin\frac{\Phi_0}{2}\sin\theta_i\sin\psi_i} + \frac{1}{\cos\frac{\Phi_0}{2}\cos\theta_i + \sin\frac{\Phi_0}{2}\sin\theta_i\sin\psi_i}\right). \quad (1)$$

$\epsilon_w(\sim 78)$, ϵ_m, ϵ_0 are the dielectric constant of a water, monolayer, and vaccuum. Φ_0 is the angle between the two legs of molecules. l is the leg length of the banana-shaped molecules. On account of hydrophobic repulsive interaction between the hydrophobic ends of banana-shaped molecules and the water surface, the geometrical constraints are imposed on the orientation of constituent banana-shaped molecules (interfacial binding effect). The geometrical constraint is taken into account by setting the limit of orientation with respect to the twist angle ψ and tilt angle as $-\psi_{\rm Max} \le \psi \le \psi_{\rm Max}$ ($\psi_{\rm Max} = \sin^{-1}(-h/(l\sin(\Phi_0/2)\sin\theta) + 1/(\tan(\Phi_0/2)\tan\theta))$) and $\theta < \theta_{\rm Max}$ ($\theta_{\rm Max} = \cos^{-1}(h/l\cos(\Phi_0/2))$) [8–10]. Here, h is the finite thickness of the two legs of constituent molecules.

In our present model, we also take into account the hard-core repulsive interaction between constituent molecules. Since the thickness of monolayers is less than the molecular length, it is sufficient to take into account the hard-core repulsive interaction between the projection of constituent banana-shaped achiral molecules [9,10]. On account of the hardcore repulsive interaction, constituent banana-shaped achiral molecules make the surface exclusive area $S_{exclusive}$, where constituent molecules cannot occupy (see Fig. 2(a)). Two interacting constituent banana-shaped molecules rarely intercross each other due to the geometry of monolayer. Thus, for simplicity, we assume that constituent molecules cannot occupy the intercrossing area S_{cross}, where constituent molecules must intercross each other to occupy the area, either. $S_{exclusive}$ and S_{cross} are represented as [10]

$$\begin{aligned} S_{exclusive}(\theta_i,\psi_i,\phi_i,\theta_j,\psi_j,\phi_j) = {} & l^2{\rm Max}\{a_z\cdot\mathbf{p}_{j+}\times(\mathbf{p}_{i+}-\mathbf{p}_{i-}), \\ & a_z\cdot\mathbf{p}_{j-}\times(\mathbf{p}_{i+}-\mathbf{p}_{i-}),0\} \\ & + l^2{\rm Max}\{a_z\cdot\mathbf{p}_{i+}\times\mathbf{p}_{j+}, a_z\cdot\mathbf{p}_{i+}\times\mathbf{p}_{j-},0\} \\ & + l^2{\rm Max}\{a_z\cdot\mathbf{p}_{j+}\times\mathbf{p}_{i-}, a_z\cdot\mathbf{p}_{j-}\times\mathbf{p}_{i-},0\} \end{aligned} \quad (2)$$

$$S_{cross}(\theta_i,\psi_i,\phi_i) = \frac{1}{2}l^2 a_z\cdot\mathbf{p}_{i+}\times\mathbf{p}_{i-} \quad (3)$$

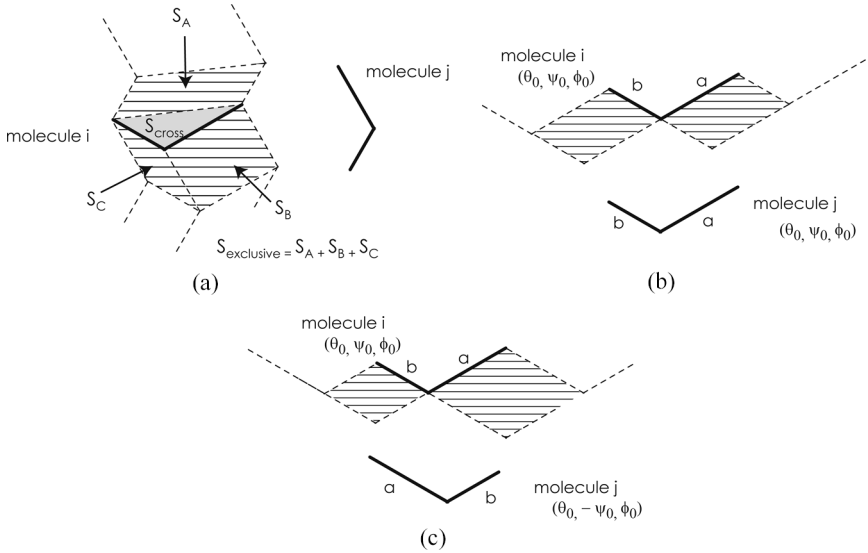

FIGURE 2 (a) An example of surface exclusive area $S_{exclusive}$ and intercrossing area S_{cross}. The two thick bent rods are the projection of constituent banana-shaped molecules, i and j onto a water surface. The surface exclusive area is $S_{exclusive} = S_A + S_B + S_C$. S_A, S_B, and S_C are the first, second, and third term of Eq. (2), respectively. (b) Surface exclusive area $S_{exclusive}$ of two interacting banana-shaped achiral molecules, i and j, with the same twist angle ψ_0, where the projection of moleculear legs onto a water surface is represented by solid rods ($\phi_0 = 0$). (c) Surface exclusive area $S_{exclusive}$ of two interacting constituent banana-shaped achiral molecules, i and j, with the different twist angle (ψ_0 and $-\psi_0$), where the projection of moleculear legs onto a water surface is represented by solid rods ($\phi_0 = 0$).

with

$$\mathbf{p}_{i+} = \left(\sin\frac{\Phi_0}{2}\cos\psi_i\cos\phi_i - \left(\cos\frac{\Phi_0}{2}\sin\theta_i + \sin\frac{\Phi_0}{2}\cos\theta_i\sin\psi_i\right)\sin\phi_i\right)a_x + \left(\sin\frac{\Phi_0}{2}\cos\psi_i\sin\phi_i + \left(\sin\frac{\Phi_0}{2}\cos\theta_i\sin\psi_i + \cos\frac{\Phi_0}{2}\sin\theta_i\right)\cos\phi_i\right)a_y$$

$$\mathbf{p}_{i-} = \left(-\sin\frac{\Phi_0}{2}\cos\psi_i\cos\phi_i - \left(\cos\frac{\Phi_0}{2}\sin\theta_i - \sin\frac{\Phi_0}{2}\cos\theta_i\sin\psi_i\right)\sin\phi_i\right)a_x + \left(-\sin\frac{\Phi_0}{2}\cos\psi_i\sin\phi_i + \left(-\sin\frac{\Phi_0}{2}\cos\theta_i\sin\psi_i + \cos\frac{\Phi_0}{2}\sin\theta_i\right)\cos\phi_i\right)a_y$$

where $\mathbf{p}_{i+}$ and $\mathbf{p}_{i-}$ are the projections of the two molecular legs $+$ and $-$ onto the water surface. $\mathbf{a}_z$ is a unit vector normal to the water surface. Max$\{X_1, X_2, X_3\}$ is the largest value among X_1, X_2, and X_3.

Calculating along the treatment of the statistical mechanics, the free energy density functional of monolayers comprised of banana-shaped achiral molecules is derived as [10]

$$\beta f[n(\Omega)] = \beta \int d\Omega n(\Omega) V(\Omega) + \int d\Omega n(\Omega) \frac{S_{cross}(\Omega)}{A} + \int d\Omega_i \int d\Omega_j n(\Omega_i) n(\Omega_j) \frac{S_{exclusive(\Omega_i,\Omega_j)}}{A} + \int d\Omega n(\Omega) \log n(\Omega). \quad (4)$$

$n(\Omega)$ is the orientational distribution of constituent molecules, where it satisfies $\int n(\Omega) d\Omega = 1$. A is the molecular area. $\beta = 1/(k_B T)$ (k_B: Boltzmann constant and T: absolute temperature). The first term is the contribution of electrostatic interaction between constituent molecules and image dipole induced at the water surface. The second and third terms are the contribution of entropy with respect to the positional distribution of constituent molecules (positional entropy) with respect to the intercrossing area and surface exclusive area, respectively. The fourth term is the contribution of entropy with respect to the orientational distribution of constituent molecules (orientational entropy).

III. COMPRESSION INDUCED CHIRAL SYMMETRY BREAKING OF MONOLAYERS COMPRISED OF BANANA-SHAPED ACHIRAL MOLECULES

In this section, we briefly describe the mechanism of the chiral-achiral phase transition of monolayers comprised of banana-shaped achiral molecules to review the importance of in-plane nematic order. The orientational distribution $n(\Omega)$ of monolayers comprised of banana-shaped achiral molecules is determined so that free energy density Eq. (4) becomes minimum. We begin our analysis from the most simple case, where the orientational distribution function $n(\Omega)$ is written by the Dirac's delta function $\delta(x)$ as

$$n_\delta(\Omega) \sin\theta_0 = \chi \delta(\theta - \theta_0)\delta(\psi - \psi_0)\delta(\phi - \phi_0) + (1 - \chi)\delta(\theta - \theta_0)\delta(\psi - \psi_0)\delta(\phi - \phi_0). \quad (5)$$

This trial function represents that the orientation (θ, ψ, ϕ) of a dominant number of constituent banana-shaped molecules is either (θ_0, ψ_0, ϕ_0) or (θ_0, $-\psi_0$, ϕ_0). $\chi/\sin\theta_0$ and $(1 - \chi)/\sin\theta_0$ are the fraction of constituent molecules with the twist angle ψ_0 and $-\psi_0$, respectively. According to Simpson [14], monolayers comprised of banana-shaped

achiral molecules form chiral structure when the orientational structure is asymmetric with respect to the twist angle ψ, i.e., $\chi \neq 1/2$. The free energy density for Eq. (5) is written as [10]

$$\beta f \sim w_{--} + (w_{++} - w_{--})\chi - 2w_{WB}\chi(1-\chi) + \chi \log \chi + (1-\chi)\log(1-\chi), \tag{6}$$

where $w_{++} = S_{exclusive}(\theta_0, \psi_0, \phi_0, \theta_0, \psi_0, \phi_0)/A$, $w_{--} = S_{exclusive}(\theta_0, -\psi_0, \phi_0, \theta_0, -\psi_0, \phi_0)/A$, $w_{+-} = S_{exclusive}(\theta_0, \psi_0, \phi_0, \theta_0, -\psi_0, \phi_0)/A$, and

$$w_{WB} = \frac{w_{++} + w_{--}}{2} - w_{+-}. \tag{7}$$

We neglect the contribution of the electrostatic interaction between the permanent dipole moments of constituent molecules and the contribution of the positional entropy with respect to the intercrossing area since they are independent of χ. The first, second, and third terms are the contributions of positional entropy with respect to the surface exclusive area. The fourth and fifth terms are the contributions of orientational entropy. w_{++} and w_{--} represent the interaction between constituent banana-shaped molecules with the same twist angles, i.e., $(\psi_i, \psi_j) = (\psi_0, \psi_0)$ or $(\psi_i, \psi_j) = (-\psi_0, -\psi_0)$. w_{+-} represents the interaction between constituent molecules with different twist angle, i.e. $(\psi_i, \psi_j) = (\psi_0, -\psi_0)$ or $(\psi_i, \psi_j) = (-\psi_0, \psi_0)$. Equation (6) is analogous to the free energy of Williams-Bragg approach [16,17]. On the analogy of Williams-Bragg approach, monolayers form achiral structure ($\chi = 1/2$) when $w_{WB} > -1$, and monolayers form chiral structure ($\chi = 0$ or $\chi = 1$) when $w_{WB} < -1$. We represents the projection lengths of two legs $+$ and $-$ of banana-shaped achiral molecules with $\psi = \psi_0$ as a and b ($a > b$), respectively (Fig. 2(b)). Then, the projection lengths of the two legs $+$ and $-$ of banana-shaped achiral molecules with $\psi = -\psi_0$ are represented as b and a, respectively. The surface exclusive areas made by two interacting banana-shaped molecules i and j with the twist angle $\psi_i = \psi_0$ and $\psi_j = \psi_0$ are depicted as the slashed areas in Figure 2(b), and the surface exclusive areas made by two interacting molecules i and j with twist angles $\psi_i = \psi_0$ and $\psi_j = -\psi_0$ are depicted as the slashed areas in Figure 2(c). The surface exclusive area of two interacting molecules with identical twist angles is roughly calculated as $S_{exclusive}(\theta_0, \psi_0, \phi_0, \theta_0, \psi_0, \phi_0) = S_{exclusive}(\theta_0, -\psi_0, \phi_0, \theta_0, -\psi_0, \phi_0) \sim 2ab$ (see Fig. 2 (b)), whereas the surface exclusive area of two interacting molecules with different twist angle is written as $S_{exclusive}(\theta_0, \psi_0, \phi_0, \theta_0, -\psi_0, \phi_0) = S_{exclusive}(\theta_0, -\psi_0, \phi_0, \theta_0, \psi_0, \phi_0) \sim a^2 + b^2$ (see Fig. 2(c)), i.e. $w_{WB} \sim -(a-b)^2/A < 0$. As molecular area A decreases during the monolayer compression, $|w_{WB}|(\propto A^{-1})$

increases. Therefore, the orientational structure of monolayers comprised of banana-shaped achiral molecules changes from achiral orientational structure ($w_{WB} > -1$) to chiral orientational structure ($w_{WB} < -1$) at the critical area A_c in the course of monolayer compression ($A_c = -(S_{exclusive}(\theta_0,\ \psi_0,\ \phi_0,\ \theta_0,\ \psi_0,\ \phi_0) + S_{exclusive}(\theta_0,\ -\psi_0,\ \phi_0,\ \theta_0,\ -\psi_0,\ \phi_0))/2 + S_{exclusive}(\theta_0,\ \psi_0,\ \phi_0,\ \theta_0,\ -\psi_0,\ \phi_0)$).

We extend this argument to more general cases, where the orientational distribution function is written by a continuous function. We write the orientational distribution function as

$$n(\Omega) = K(\Omega) e^{-\beta V(\Omega) - \frac{S_{cross}(\Omega)}{A}}, \tag{8}$$

where $K(\Omega)$ represents the contribution of the positional entropy with respect to the surface exclusive area $S_{exclusive}$ and the orientational entropy. $K(\omega)$ is expressed by the sum of even function part $\mathcal{E}(\Omega)$ and odd function part $\epsilon\mathcal{O}(\Omega)$ with respect to the twist angle ψ as

$$K(\Omega) = \mathcal{E}(\Omega) + \mathcal{EO}(\Omega), \tag{9}$$

where $\mathcal{E}(\Omega) \equiv (K(\theta,\psi,\phi) + K(\theta,-\psi,\phi))/2$ and $\epsilon\mathcal{O}(\Omega) \equiv (K(\theta,\psi,\phi) - K(\theta,-\psi,\phi))/2$. Note that monolayers comprised of banana-shaped achiral molecules form chiral structure when the orientational distribution is asymmetric with respect to the twist angle ψ, i.e., $\epsilon\mathcal{O}(\Omega) \neq 0$, since $\exp(-\beta V(\Omega) - S_{cross}(\Omega)/A)$ is an even function of ψ. At the vicinity of the critical area A_c ($\epsilon\mathcal{O}(\Omega) << \mathcal{E}(\Omega)$), the free energy density of monolayers comprised of banana-shaped achiral molecules is approximately written as [10]

$$\begin{aligned}\beta f \sim & \int d\Omega \mathcal{E}(\Omega) \log \mathcal{E}(\Omega) e^{-\beta V(\Omega) - \frac{S_{cross}(\Omega)}{A}} \\ & + \int d\Omega \int d\Omega' \mathcal{E}(\Omega)\mathcal{E}(\Omega') \frac{S_{exclusive}(\Omega,\Omega')}{A} \\ & \quad \times e^{-\beta V(\Omega) - \beta V(\Omega') - \frac{S_{cross}(\Omega)}{A} - \frac{S_{cross}(\Omega')}{A}} \\ & + \frac{\epsilon^2}{2}(1+w) \int d\Omega \frac{\mathcal{O}(\Omega)^2}{\mathcal{E}(\Omega)} e^{-\beta V(\Omega) - \frac{S_{cross}(\Omega)}{A}},\end{aligned} \tag{10}$$

with

$$w = \frac{1}{A} \frac{2 \int d\Omega \int d\Omega' \mathcal{O}(\Omega)\mathcal{O}(\Omega') S_{exclusive}(\Omega,\Omega') e^{-\beta V(\Omega) - \beta V(\Omega') - \frac{S_{cross}(\Omega)}{A} - \frac{S_{cross}(\Omega')}{A}}}{\int d\Omega \frac{\mathcal{O}(\Omega)^2}{\mathcal{E}(\Omega)} e^{-\beta V(\Omega) - \frac{S_{cross}(\Omega)}{A}}}. \tag{11}$$

The first and second terms are the contribution of the even function part of $K(\Omega)$. The third term is the contribution of the odd function part

of $K(\Omega)$. Equation (10) indicates that monolayers form a chiral orientational structure when $w < -1$, and that monolayers form an achiral orientational structure when $w > -1$. Actually, the physical meaning of w is equivalent to that of w_{WB}. In other words, our present treatment extends the Williams-Bragg approach to the general orientational distribution. We represent $\mathcal{E}(\Omega)$ and $\epsilon\mathcal{O}(\Omega)$ by Fourier series as $\mathcal{E}(\Omega) = a_0(\theta,\phi)/2 + \Sigma_n a_n(\theta,\phi)\cos 2\psi$ and $\epsilon\mathcal{O}(\Omega) = \Sigma_n b_n(\theta,\phi)\sin 2\psi$ $(a_0/2 \geq \Sigma_n |a_n(\theta,\phi)|)$. The orientational entropy contributes to form random orientational distribution ($K(\Omega) = constant$), and positional entropy with respect to the surface exclusive area contributes to form chiral orientational structure $\mathcal{O} \neq 0$ as we have discussed. Hence, we calculate w value numerically for the most simple trial function $\mathcal{E} = a_0^c$ and $\epsilon\mathcal{O} = b_1^c \sin 2\psi$ (a_0^c and b_1^c are constants) as a function of molecular area A for several l, Φ_0, and coupling constant $\alpha(\equiv \mu_0^2/(16\pi l^3 \epsilon_0 \epsilon_m k_B T) \cdot (\epsilon_w - 1)/(\epsilon_w + 1))$ [10]. However, we could not find the critical area A_c, where $w = -1$, in the region $A > 10\,\text{Å}^2$ [10]. We, then, considered the possibilities that the formation of chiral orientational structure is enhanced by the in-plane nematic ordering, and calculated w values numerically for $\mathcal{E} = a_0^{c'}$ and $\epsilon\mathcal{O} = b_1^{c'} \cos 2\phi \sin 2\psi$ ($a_0^{c'}$ and $b_1^{c'}$ are constants). The w values of monolayers comprised of banana-shaped achiral molecules with $l = 15\,\text{Å}$, $\Phi_0 = 120^\circ$, and $\alpha = 0.001$, where it is corresponding to e.g., $\mu_0 = 1.65\,\text{D}$ and $\epsilon_m \sim 2$, are plotted by the solid curve in Figure 3 as

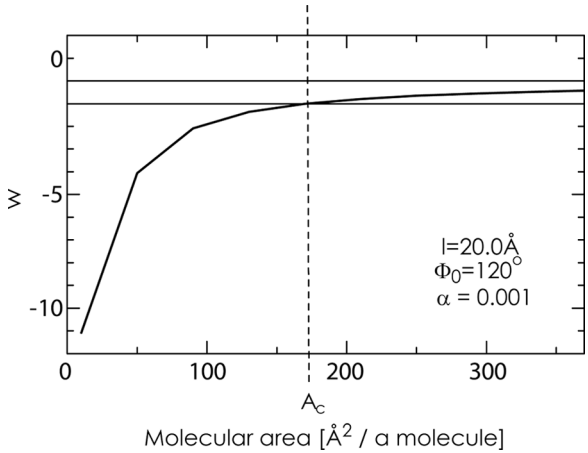

FIGURE 3 Model calculation of w when we assume $b_1(\theta,\phi)$ is constant. w is calculated for monolayers of banana-shaped achiral molecules with $l = 20$ Å, $\Phi_0 = 120^\circ$, and $\alpha = 0.001$.

a function of molecular area A. Results of numerical calculation of w values for monolayers with several l, Φ_0, and α values are discussed in Ref. [10]. The w value becomes -1 at the critical area $A_c \sim 170\,\text{Å}^2$. This calculation demonstrates that the orientational structure of monolayers comprised of banana-shaped molecules change from achiral orientational structure to chiral orientational structure in the course of a monolayer compression, and that the in-plane nematic order plays an important role in the achiral-chiral phase transition.

IV. COMPRESSION INDUCED IN-PLANE NEMATIC ORDERING OF MONOLAYERS COMPRISED OF BANANA-SHAPED ACHIRAL MOLECULES

In sec. III we discussed that in-plane nematic order plays an important role in the formation of chiral structure of banana-shaped achiral molecules. Here, we discuss the in-plane nematic ordering of monolayers comprised of banana-shaped achiral molecules using the free energy density functional, Eq. (4) in a manner similar to Onsager's theory of isotropic-nematic transition of bulk liquid crystal. To begin with, we consider the most simple case, where the orientational distribution function is written as

$$2n(\Omega)\sin\theta_0 = \nu\delta(\theta-\theta_0)\delta(\psi)(\delta(\phi-0)+\delta(\phi-\pi)) + (1-\nu)\delta(\theta-\theta_0)\delta(\psi)(\delta(\phi-\pi/2)+\delta(\phi+\pi/2)). \quad (12)$$

This trial function represents that the orientation (θ, ψ, ϕ) of a dominant number of constituent molecules is (θ_0, 0, 0), (θ_0, 0, π), or (θ_0, 0, $\pm\pi/2$). Since the in-plane nematic order parameter does not depend on the difference between the number of molecules with $\phi = 0$ ($\pi/2$) and the number of molecules with $\phi = \pi(-\pi/2)$, we simply assume that the number of molecules with $\phi = 0$ ($\pi/2$) equals to the number of molecules with $\phi = \pi$ ($-\pi/2$). $\phi = 0$, π and $\phi = \pm\pi/2$ are representatives of constituent molecules with different tilt azimuth orientation. $\delta(\psi)$, i.e., a dominant number of constituent molecules possess zero twist angle $\psi = 0$, represents the monolayers are achiral. This treatment is also used in the Onsager's theory. $\nu/\sin\theta_0$ is the fraction of molecules with $\phi = 0$ or π, and $(1-\nu)/\sin\theta_0$ is the fraction of molecules with $\phi = \pi/2$ or $-\pi/2$. Substituting Eq. (12) into Eq. (4), the free energy density is written as

$$\beta f \sim w^N_{--} + (w^N_{++} - w^N_{--})\nu - 2w^N_{WB}\nu(1-\nu) + \nu\log\nu + (1-\nu)\log(1-\nu), \quad (13)$$

where $w^N_{++} = (S_{exclusive}(\theta_0, 0, 0, \theta_0, 0, 0) + S_{exclusive}(\theta_0, 0, 0, \theta_0, 0, \pi))/A$, $w^N_{--} = (S_{exclusive}(\theta_0, 0, \pi/2, \theta_0, 0, \pi/2) + S_{exclusive}(\theta_0, 0, \pi/2, \theta_0, 0, -\pi/2))/A$, $w^N_{+-} = (S_{exclusive}(\theta_0, 0, 0, \theta_0, 0, \pi/2) + S_{exclusive}(\theta_0, 0, 0, \theta_0, 0, -\pi/2))/A$ and

$$w^N_{WB} = \frac{w^N_{++} + w^N_{--}}{2} - w^N_{+-}. \tag{14}$$

The first, second, and third terms are the contributions of positional entropy with respect to the surface exclusive area $S_{exclusive}$. The fourth and fifth terms are the contributions of orientational entropy. w^N_{++} and w^N_{--} represent the interactions between the constituent molecules, whose orientations of ξ-axis projections are parallel to each other, and w^N_{+-} represent the interaction between the constituent molecules, whose orientations of ξ-axis projections are perpendicular to each other. The contributions of electrostatic interaction between the permanent dipole moments of constituent molecules and image dipoles induced at the water surface, and positional entropy with respect to the intercrossing area S_{cross} are neglected since they are independent of ν. Equation (13) is again analogous to the free energy of Williams-Bragg approach. On the analogy of Williams-Bragg approach, when $w^N_{WB} > -1$, monolayers are in isotropic phase ($\nu = 1/2$), whereas, when, $w^N_{WB} < -1$, monolayers are in in-plane nematic phase ($\nu = 0$ or 1). The surface exclusive area is depicted as the slashed area in Figures 4(a) and (b). The angle between the projections of two molecular legs is represented by $\Delta(= 2\tan^{-1}(\tan(\Phi_0/2)/\sin\theta_0))$, and the length of the projections of molecular legs is represented by a. When the ξ-axis projections of two interacting molecules are parallel to each other (see Fig. 4(a)), $S_{exclusive}(\theta_0, 0, 0, \theta_0, 0, 0) = S_{exclusive}(\theta_0, 0, 0, \theta_0, 0, \pi) = S_{exclusive}(\theta_0, 0, \pi/2, \theta_0, 0, \pi/2) = S_{exclusive}(\theta_0, 0, \pi/2, \theta_0, 0, -\pi/2) = 4a^2 \sin(\Delta/2)\cos(\Delta/2)$. When the ξ-axis projections of two interacting molecules are perpendicular to each other (see Fig. 4(b)), $S_{exclusive}(\theta_0, 0, 0, \theta_0, 0, \pi/2) = S_{exdustve}(\theta_0, 0, 0, \theta_0, 0, -\pi/2) = 4a^2 \sin^2(\Delta/2)$. We assume that constituent banana-shaped achiral molecules have $\Phi_0 \sim 120^\circ$ ($\Phi_0 \geq \pi/2$ rad), where it is a typical value of banana-shaped achiral molecules used in the studies of liquid crystals [11]. The angle between the two leg projections of such banana-shaped achiral molecules is $\Delta \geq \Phi_0 (\geq \pi/2)$, i.e., $w^N_{WB} \sim -4\sqrt{2a^2}\sin(\Delta/2)\sin(\Delta/2 - \pi/4)/A < 0$. As the molecular area A decreases during the monolayer compression, $|w^N_{WB}| (\propto A^{-1})$ increases. Hence, in the course of monolayer compression, monolayers comprised of banana-shaped achiral molecules change from isotropic phase ($\nu = 1/2$) to in-plane nematic phase ($\nu = 0$ or 1) at the critical area A^N_c, where $w^N_{WB} = -1 (A^N_c = 4a^2 \tan(\Delta/2)(\tan(\Delta/2) - 1)/(1 + \tan^2(\Delta/2)))$. We discussed the presence of in-plane nematic phase using the similar

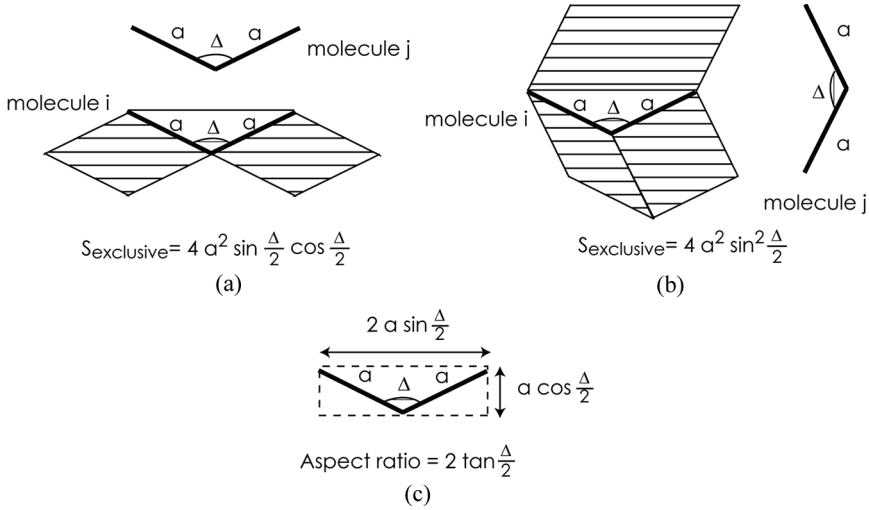

FIGURE 4 (a) The surface exclusive area $S_{exclusive}$ of two interacting molecules, i and j, whose ξ-axis projections are parallel to each other ($\theta = \theta_0$ and $\psi = 0$). Projections of molecular legs are represented by the solid rods. (b) Surface exclusive area $S_{exclusive}$ of two interacting molecules, i and j, whose ξ-axis projections are perpendicular to each other. Projections of molecular legs are represented by the solid rods (ϕ_0). (c) Projection of a constituent banana-shaped molecules viewed as an effective rod-shaped molecules with aspect ratio $2\tan(\Delta/2)$ (dashed rectangular).

argument to sec. III. However, there is an important difference. The compression induced chiral symmetry breaking of monolayers comprised of banana-shaped molecules is attributed to the difference of projection shapes between constituent molecules with $\psi = \psi_0$ and constituent molecules with $\psi = -\psi_0$. On the other hand, in-plane nematic ordering originates from the elongated shape of banana-shaped molecules (see Fig. 4(c)). Therefore, both in-plane nematic order and chiral orientational structure originate from the banana shape of constituent molecules. The projected shapes of constituent banana-shaped achiral molecules are roughly viewed as rectangular shape depicted by dashed line in Figure 4(c), whose aspect ratio is $2\tan(\Delta/2)$. Δ is dependent on the tilt angle θ_0. Thus, constituent banana-shaped achiral molecules apparently behave as rod-shaped molecules, whose aspect ratio is dependent on the orientation, in the 2D geometry of monolayers.

We extend the argument to more general case, where $n(\Omega)$ is represented by a continuous function. $n(\Omega)$ is written as Eq. (8). $K(\Omega)$ is

further represented as

$$K(\Omega) = \mathcal{I}(\Omega) + \epsilon\mathcal{N}(\Omega), \tag{15}$$

where $\mathcal{I}(\Omega) = 1/(2\pi)\int_{-\pi}^{\pi} d\phi\, K(\Omega)$ and $\epsilon\mathcal{N}(\Omega) = K(\Omega) - 1/(2\pi)\int_{-\pi}^{\pi} d\phi\, K(\Omega)$. $\mathcal{I}$ and $\epsilon\mathcal{N}$ are the ϕ-independent part and ϕ-dependent part of $K(\Omega)$, respectively. Monolayers are in isotropic phase when $\epsilon\mathcal{N} = 0$, whereas monolayers are in in-plane nematic phase when $\epsilon\mathcal{N} \neq 0$. At the vicinity of critical area A_c^N of isotropic-in-plane nematic phase transition, $\epsilon\mathcal{N} << \mathcal{I}$ is satisfied, and the free energy density functional is approximately written as

$$\begin{aligned}\beta f \sim & \int d\Omega \mathcal{I}(\Omega)\, \log \mathcal{I}(\Omega) e^{-\beta V(\Omega) - \frac{S_{cross}(\Omega)}{A}} \\ & + \int d\Omega_i \int d\Omega_j \mathcal{I}(\Omega_i)\mathcal{I}(\Omega_j) \frac{S_{exclusive}(\Omega_i, \Omega_j)}{A} e^{-\beta V(\Omega_i) - \frac{S_{cross}(\Omega_i)}{A}} \\ & \times e^{-\beta V(\Omega_j) - \frac{S_{cross}(\Omega_j)}{A}} + \frac{\epsilon^2}{2}(1 + w^N) \int d\Omega \frac{\mathcal{N}^2\Omega}{\mathcal{I}(\Omega)} e^{-\beta V(\Omega) - \frac{S_{cross}(\Omega)}{A}},\end{aligned} \tag{16}$$

with

$$w^N = \frac{2}{A} \frac{\int d\Omega_j \int d\Omega_j \mathcal{N}(\Omega_i)\mathcal{N}(\Omega_j) S_{exclusive(\Omega_i,\Omega_j)} e^{-\beta V(\Omega_i) - \frac{S_{cross}(\Omega_i)}{A}} e^{-\beta V(\Omega_j) - \frac{S_{cross}(\Omega_j)}{A}}}{\int d\Omega \frac{\mathcal{N}^2(\Omega)}{\mathcal{I}(\Omega)} e^{-\beta V(\Omega) - \frac{S_{cross}(\Omega)}{A}}}. \tag{17}$$

When $w^N > -1$, $\epsilon\mathcal{N} = 0$, i.e., monolayers are in isotropic phase, while when $w^N < -1$, $\epsilon\mathcal{N} \neq 0$, i.e., monolayers are in in-plane nematic phase. The physical meaning of w^N is equivalent to that of w_{WB}^N. Actually, w^N is reduced to w_{WB}^N when we substitute Eq. (12) into Eq. (17). We again express $\mathcal{I}$ and $\epsilon\mathcal{N}$ by Fourier series as $\mathcal{I}(\Omega) = c_0(\theta, \psi)$ and $\epsilon\mathcal{N}(\Omega) = \sum_{n=1}^{N} c_n(\theta, \psi) \cos n\phi$. When any of $c_{n\neq 0}(\theta, \psi)$ is non-zero, monolayers possess in-plane nematic order. $K(\Omega)$ represents the contributions of orientational entropy and positional entropy with respect to the surface exclusive area $S_{exclusive}$ to the orientational distribution function. As we have already discussed, the orientational entropy contributes to form the random orientational distribution, whereas the positional entropy with respect to $S_{exclusive}$ contributes to form the in-plane nematic ordering. Thus, for simplicity, we begin our numerical calculation using a trial function $\mathcal{I} = c_0^c$ and $\epsilon\mathcal{N} = c_2^c \cos 2\phi$, where c_0^c and c_2^c are constants. w^N of monolayers comprised of banana-shaped achiral molecules with $l = 20.0$ Å, $\Phi_0 = 120^\circ$, and $\alpha = 0.001$ is calculated as a function of A numerically, and plotted to the solid curves in Figures 5(a)–(c). The solid curves in Figures 5(a)–(c)

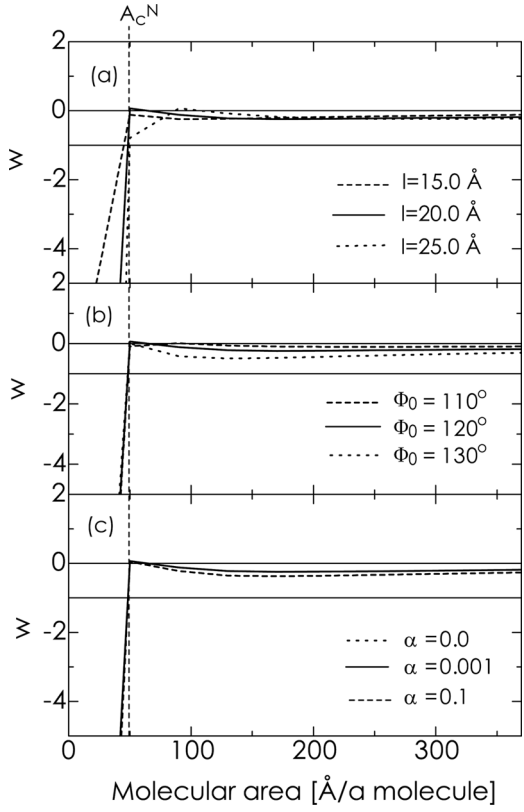

FIGURE 5 Model calculation of w_N when $\mathcal{I} \sim c_0^c$ and $\epsilon\mathcal{N} \sim c_2^c \cos 2\phi$. The solid curves are w_N of monolayers with $l = 20.0$ Å, $\Phi_0 = 120^\circ$, and $\alpha = 0.001$ as a function of A. w_N is also calculated for various l, Φ_0, and α in (a), (b), and (c), respectively. The roughness of the curves at the small molecular area is because the number of plotted points are few.

are equivalent. This result indicates that in-plane nematic ordering occurs at the critical area $A_c^N \sim 50$ Å^2 (the area with $w^N = -1$), where it is smaller area than the critical area of chiral symmetry breaking. w^N is calculated for several l, Φ_0, and α (see Fig. 5). However, the results does not change so much from the solid line ($l = 20.0$ Å, $\Phi_0 = 120^\circ$, and $\alpha = 0.001$). As we have discussed in sec.III, the twist angle ψ can change the shape of projections of constituent molecules. In our previous study, we found that the monolayers form the orientational distribution proportional to cos 2ψ from large molecular area ($A > 300$ Å^2) in a monolayer compression (see Fig. 5 in Ref. [10]).

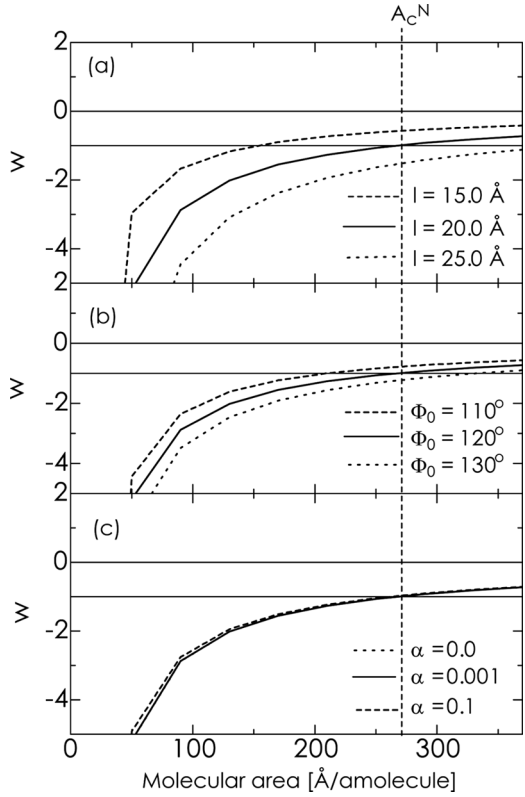

FIGURE 6 Model calculation of w^N when $\mathcal{I} \sim c_0^c$ and $\epsilon\mathcal{N} \sim c_2^c \cos 2\psi \cos 2\phi$. The solid curves are w^N of monolayers with $l = 20.0$ Å, $\Phi_0 = 120.0^\circ$, and $\alpha = 0.001$ as a function of A. w^N is also calculated for various l, Φ_0, and α in (a), (b), and (c), respectively. The roughness of the curves at the small molecular area is because the number of plotted points are few.

In order to investigate the possibilities that the twist angle ψ contributes to the formation of in-plane nematic phase, we also consider a trial function $\mathcal{I} \sim c_0^{c'}$ and $\epsilon\mathcal{N} \sim c_2^{c'} \cos 2\psi \cos 2\phi$ and ($c_0^{c'}$ and $c_2^{c'}$ are constants). w^N of monolayers comprised of banana-shaped achiral molecules with $l = 20.0$ Å, $\Phi_0 = 120^\circ$, and $\alpha = 0.001$ is calculated as a function of A numerically, and plotted to the solid curves in Figures 6(a)–(c). The solid curves in Figures 6(a)–(c) are equivalent. This result indicates that isotropic-in-plane nematic transition occurs at the critical area $A_c \sim 270$ Å^2, where it is larger than the critical area of the chiral symmetry breaking. When we extend the discussion of Eq. (12) to banana-shaped molecules with finite twist angle ($\psi \neq 0$),

banana-shaped achiral molecules are viewed as effective rod-shaped molecules with aspect ratio $\min\{2/(\cos\theta_i \tan\psi_i + \sin\theta_i(\tan(\Phi_0/2)\cos\psi_i)), 2/(-\cos\theta_i \tan\psi_i + \sin\theta_i/(\tan(\Phi_0/2)\cos\psi_i))\}$, where $\min\{A, B\}$ is the smaller value of A and B. The aspect ratio of effective rod-shaped molecules becomes maximum when $\psi = 0$ and $\pm\pi/2$. Therefore, the orientational distribution proportional to $\cos 2\psi$ is the origin of the in-plane nematic ordering. Constituent banana-shaped achiral molecules behave as rod-shaped molecules with variable aspect ratio in 2D geometry. In-plane nematic ordering largely increases positional entropy when the projections of constituent molecules have large aspect ratio, i.e., in the presence of the orientational distribution proportional to $\cos 2\psi$. On the other hand, the chiral orientational distribution $\sin 2\psi$ increases the constituent molecules with finite twist angle orientation ($\psi \neq 0$) and decreases the constituent molecules with large aspect ratio. The in-plane nematic order increases larger positional entropy than the formation of chiral structure. Consequently, monolayers comprised of banana-shaped achiral molecules form in-plane nematic phase at the larger molecular area than the formation of chiral symmetry breaking. Experimentally, as we discussed in sec.I, BAR and SHG are capable of probing the in-plane nematic ordering and chiral symmetry breaking of monolayers. On the measurement of BAR and SHG during the monolayer compression, it is possible to check the prediction of present theory that in-plane nematic order is established in a larger molecular area than chiral symmetry breaking. Our present results indicate that constituent banana-shaped achiral molecules behave as rod-shaped molecules with variable aspect ratio and monolayers comprised of banana-shaped achiral molecules form in-plane nematic order at the larger molecular area than the formation of chiral orientational structure.

V. CONCLUSION

The orientational structure of monolayers comprised of banana-shaped achiral molecules has been analyzed in the context of chiral formation and in-plane nematic phase formation, taking into account the electrostatic interaction between the permanent dipole moments of constituent molecules and image dipoles induced at the water surface, and hard-core repulsive interaction between constituent molecules. The free energy density functional of the monolayers has been derived as a generalization of Williams-Bragg approach. On the analogy of Williams-Bragg approach, it has been demonstrated that monolayers comprised of banana-shaped achiral molecules form chiral orientational structure during the monolayer compression due to the

2D geometry of monolayers and that in-plane nematic order enhances the achiral-chiral phase transition. In a similar framework, we demonstrated that banana-shaped achiral molecules were viewed as effective rod-shaped molecules with variable aspect ratio and that in-plane nematic order was established at a larger molecular area than the achiral-chiral phase transition in the course of a monolayer compression. In conclusion, the in-plane nematic order plays an important role in the formation of chiral orientational structure.

REFERENCES

[1] Gaines, G. L. (1966). *Insoluble Monolayers at Liquid-Gas Interfaces*, Interscience: New York.
[2] Kaganer, V. M., Mohwald, H., & Dutta, P. (1999). *Rev. Mod. Phys.*, *71*, 779.
[3] de Gennes, P. G. & Prost, J. (1995). *The Physics of Liquid Crystals*, Clarendon Press: Oxford.
[4] Iwamoto, M. & Wu, C. X. (2000). *The Physical Properties of Organic Monolayers*, World Scientific: Singapore.
[5] Tojima, A., Manaka, T., & Iwamoto, M. (2001). *J. Chem. Phys.*, *115*, 9010.
[6] Iwamoto, M., Wu, C. X., & Zhao, W. (2000). *J. Chem. Phys.*, *119*, 2880.
[7] Fujimaki, H., Manaka, T., Ohtake, H., Tojima, A., & Iwamoto, M. (2003). *J. Chem. Phys.*, *119*, 7427.
[8] Yamamoto, T., Oguchi, S., Manaka, T., & Iwamoto, M. (2006). *Thin Solid Films*, *499*, 242.
[9] Yamamoto, T., Manaka, T., & Iwamoto, M. (2006). *Colloids and Surfaces A: Physicochem. Eng. Aspects*, *284–285*, 154.
[10] Yamamoto, T., Manaka, T., Taguchi, D., & Iwamoto, M. (2006). *J. Chem. Phys.*, *125*, 034704.
[11] Pelzl, G., Diele, S., & Weissflog, W. (1999). *Adv. Mater.*, *11*, 707.
[12] Niori, T., Sekine, T., Watanabe, J., Furukawa, T., & Takezoe, H. (1996). *J. Mater. Chem.*, *6*(7), 1231.
[13] Link, D. R., Natale, G., Shao, R., Maclennan, J. E., Clark, N. A., Korblova, E., & Walba, D. M. (1997). *Science*, *278*, 1924.
[14] Simpson, G. J. (2002). *J. Chem. Phys.*, *117*, 3398.
[15] Onsager, L. (1949). *Am. (N.Y.) Acad. Sci.*, *51*, 627.
[16] Iwamoto, M., Wu, C. X., Ou-Yang, Z. C. (1999). *Phys. Rev. E*, *59*, 586.
[17] Zhao, W., Wu, C. X., & Iwamoto, M. (2000). *Phys. Rev. E*, *61*, 6669.